

Bayesian Estimation of Multivariate Hawkes Processes with Inhibition and Sparsity

Isabella Deutsch¹ and Gordon J. Ross¹
isabella.deutsch@ed.ac.uk gordon.ross@ed.ac.uk

¹University of Edinburgh

January 14, 2022

Abstract

Hawkes processes are point processes that model data where events occur in clusters through the self-exciting property of the intensity function. We consider a multivariate setting where multiple dimensions can influence each other with intensity function to allow for excitation and inhibition, both within and across dimensions. We discuss how such a model can be implemented and highlight challenges in the estimation procedure induced by a potentially negative intensity function. Furthermore, we introduce a new, stronger condition for stability that encompasses current approaches established in the literature. Finally, we examine the total number of offsprings to reparametrise the model and subsequently use Normal and sparsity-inducing priors in a Bayesian estimation procedure on simulated data.

Keywords: Intensity Function, Interpretation, Prior Choice, Stability

1 Introduction

Classic Hawkes processes (Hawkes, 1971) are point processes capturing the self-exciting behaviours of events that occur in clusters or bursts. A prominent application is found in the earthquake literature, where large earthquakes trigger subsequent aftershocks (Ogata, 1988). Hawkes processes are successfully used in a variety of other settings that share this self-excitation nature: crime and terror modelling (Mohler, 2013; Shelton et al., 2018; Tucker et al., 2019), accidents (Kalair et al., 2021), stock market tradings (Rambaldi et al., 2017), and social media (Lai et al., 2016).

For each event from a point process process we record the time when it happened $Y = (t_1 \dots t_N) \in [0, T_{max}]$, such that t_i is the event time at which the i^{th} event took

place. The self-exciting linear Hawkes process is defined by its conditional intensity function $\lambda(t|Y^t, \Theta)$, which at time t is conditional on the previous events $Y^t = \{t_i : t > t_i\}$ (Hawkes, 1971) and parameters Θ used to specify the parametric form of intensity. For convenience of notation the dependence on Y^t and Θ is suppressed further on.

The following specification encompasses the self-exciting nature:

$$\lambda(t|Y^t, \Theta) = \mu(t) + \sum_{i:t>t_i} K g(t - t_i) \quad (1)$$

Here, $\mu(\cdot) > 0$ is the background rate that can capture seasonality and underlying trends. We call $K g(\cdot)$ the excitation kernel, where $K \geq 0$, $g(x) \geq 0$ for $x \geq 0$ and $\int_0^\infty g(x) dx = 1$. Each observation prior to t contributes to the intensity at time t as governed by the kernel. This drives the self-exciting behaviour of the Hawkes process. Both the background rate and the kernel depend on parameters $\Theta = (\Theta_\mu, K, \Theta_g)$ where Θ_μ and Θ_g contains all parameters from $\mu(\cdot) > 0$ and $g(\cdot)$, respectively. To estimate them, a plethora of methods is successfully employed in the literature, for example maximum likelihood approaches and Bayesian methods (Veen and Schoenberg, 2008; Rasmussen, 2013; Guo et al., 2018; Chen and Stindl, 2018).

1.1 Paper Overview

The remainder of this paper is organised as follows. Section 2 reviews the M -dimensional Hawkes process with corresponding sparsity and the branching structure interpretation. In Section 3 we describe the multivariate Hawkes process with inhibition alongside considerations to ensure a non-negative intensity. Section 4 discusses two aspects regarding the model implementation. First, we introduce a new, stronger conditions for stability, which is compared to two current approaches from the literature. Second, we highlight challenges when integrating the intensity function. In Section 5 we examine Normal and sparsity priors based on a reparametrisation of the multivariate Hawkes processes. Section 6 summarises the posterior inference and Section 7 presents an example on simulated data using the aforementioned aspects. We finish with a discussion and comments on future work in Section 8.

2 Background

This section considers the M -dimensional Hawkes process and summarises approaches for sparse estimation procedures. Moreover, we examine how the Hawkes process can be written as a superposition of Poisson processes that allow for a branching interpretation.

2.1 Multivariate Hawkes Process

The model presented in Equation 1 extends to an M -dimensional linear Hawkes process incorporating both self-excitation and cross-excitation. This is called a multivariate linear Hawkes process. Assume that there are M dimensions with event times $Y_1 = (t_{11} \dots t_{1N_1})$ in dimension 1 to event times $Y_M = (t_{M1} \dots t_{MN_M})$ in dimension M . At time t the intensity in dimension i is :

$$\lambda_i(t) = \mu_i(t) + \sum_{j=1}^M \sum_{l:t>t_{jl}} K_{ji} g_{ji}(t - t_{jl}) \quad (2)$$

For the remainder of this paper we consider the background rate to be constant in each dimension: $\mu_i(x) = \mu_i$ and write $\mu = (\mu_1 \dots \mu_M)$. Moreover, we assume the following form for the excitation kernel for all i, j : $g_{ij}(x) \geq 0$ for $x \geq 0$ and $\int_0^\infty g_{ij}(x) dx = 1$. Here, $K_{ij} \geq 0$ describes the excitation effect an event in dimension i has on dimension j . We write $\mathbf{K} = \{K_{ij}\}$ where $i, j = 1 \dots M$.

For any multivariate point process the likelihood for data Y is (Daley and Vere-Jones, 2003, p. 23):

$$p(Y|\Theta) = \prod_{m=1}^M \prod_{i=1}^{N_m} \lambda_m(t_i|\theta) \exp(-\Lambda) \quad (3)$$

where $\Lambda = \sum_{m=1}^M \int_0^{T^{max}} \lambda_m(x|\Theta) dx$ and $\Theta = (\mu, \mathbf{K}, \Theta_g)$. Here, Θ_g contains all parameters from $g_{ij}(\cdot)$ for all $i, j = 1 \dots M$. Note that the evaluation of both the likelihood and the log-likelihood require Λ , which is the integral of the intensity function.

2.2 Sparsity

Many real life problems of multivariate Hawkes processes also contain sparsity in \mathbf{K} (e.g. Eichler et al., 2017). For our example (Section 7) we make use of this concept through sparsity-inducing priors (Section 5.3). There are multiple successful cases of sparsity application available in the literature. Xu et al. (2016) use group Lasso and the EM-Algorithm to uncover the entries of \mathbf{K} that are truly zero. Two-step procedure are a common workaround to uncover those structural zeros. Yu et al. (2020) separate the learning of the structure and the estimation of the non-zero parameters. Similarly, Miscouridou et al. (2018) use elaborate hierarchical structures and prior specifications to uncover sparsity, heterogeneity, reciprocity, and community structure in their multivariate Bayesian estimation procedure. Both methods only provide an approximation to the parameters (or their posterior distributions).

2.3 Branching Interpretation

We now examine how data from a one-dimensional linear Hawkes process can be related to an underlying branching structure as we utilise this concept in Section 5.1 to motivate a new parametrisation. We discuss here the common branching structure interpretation when $K > 0$.

The model in Equation 1 can be written as the superposition of Poisson processes (Hawkes and Oakes, 1974) such that the intensity function is a sum of independent Poisson processes. Suppose that j events $(t_1 \dots t_j)$ happened before time t . Then the intensity at time t is the sum of the background process $\mu(t)$ and j offspring processes with intensities $K g(t-t_j)$, where each offspring process was *triggered* by a previous event. This gives rise to the following branching structure interpretation of a Hawkes process (Daley and Vere-Jones, 2003, p. 202). Data generated from an excitation-only Hawkes process consists of two types of events that come from distinct Poisson processes, where each event is generated by exactly one process (Rasmussen, 2013):

1. *Immigrant events* come from the background process with intensity $\mu(t)$.
2. *Offspring events* come from an offspring process which had been triggered by a previous event. Here, each event has an average of K *direct* offsprings if $T_{max} \rightarrow \infty$.

Note that offspring events trigger offspring processes as well. This can lead to *cascades* started by an immigrant event that has offspring events, which, in turn, has offspring events etc. Figure 1 visualises this branching structure. This concept will be utilised in Section 5.1 to introduce a new parametrisation based on the total number of offsprings.

While it is not known whether an event is an immigrant or offspring for a given data set, this perspective nevertheless can be exploited for sampling, inference, and interpretation. These interpretations hold asymptotically for $T_{max} \rightarrow \infty$. For finite T_{max} some offspring events may be larger than T_{max} and therefore would not be included in a simulated data set. Such edge effects are common in the Hawkes literature and diminish when T_{max} is large (Daley and Vere-Jones, 2003, p. 275).

This interpretation extends to the excitation multivariate case (all entries of \mathbf{K} positive) where an event in dimension i triggers offspring processes in all dimensions j . In turn, resulting offspring events can trigger offspring processes in all dimensions. Hence, cascades can potentially lead through different dimensions, which all contribute to the total number of offsprings of the immigrant event that started the cascade, which is discussed in Section 5.1.

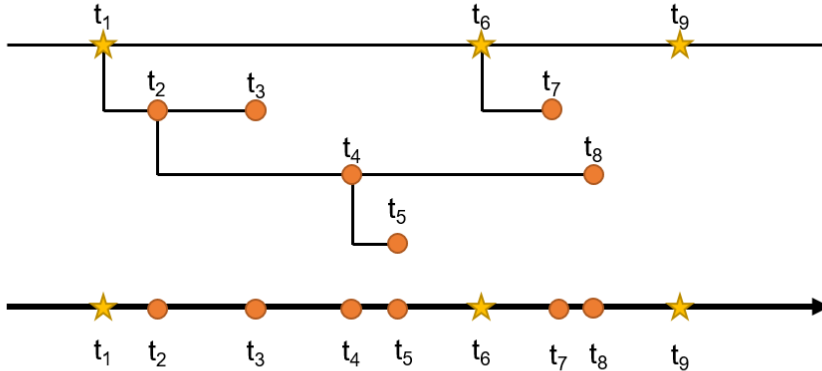


Figure 1: Sketch of the branching structure interpretation in one dimension. In this example (t_1, t_6, t_9) are the immigrant events, indicated by a star on the top and the summarised timeline below. The event t_1 has two *direct* offsprings, namely t_2 and t_3 . The former has further offsprings. For example t_1 has a total of five offsprings (number of offspring events in the cascade that started in t_1), whereas t_9 has none.

3 Multivariate Hawkes Process with Inhibition

This section discusses the multivariate Hawkes process under both excitation and inhibition. After the model set up we review approaches to ensure a non-negative intensity function and focus on the specifications of a link function.

While most examples of a Hawkes process just modelling excitation (each $K_{ij} \geq 0$), Hawkes processes also capture both excitation and inhibition when each $K_{ij} \in \mathbb{R}$. Hence, the occurrence of an event in dimension i can increase or decrease the intensity function in each dimension $j = 1 \dots M$. This is a substantial extension of the specification outlined in Equation 2, which has received less attention in the literature.

A prominent application of Hawkes processes with inhibition can be found in neural spike trains, where the inhibition captures the period of decreased intensity after a neural spike event (Eichler et al., 2017). Moreover, such models have been successful employed in a variety of fields, such as financial applications (Lu and Abergel, 2018; Teterova, 2018) or in adequately modelling the popular MemeTracker data set (Lemonnier and Vayatis, 2014).

Other approaches for inhibition are also suggested in the literature, for example Apostolopoulou et al. (2019) base their approach on a multiplicative thinning factor, which leads to a separate strand of work beyond of the standard Hawkes Process set up. For this paper we only consider inhibition through negative K_{ij} .

3.1 Model

The intensity of a M -dimensional Hawkes process with inhibition at time t in dimension i is:

$$\lambda_i(t) = \mu_i + \sum_{j=1}^M \sum_{l:t>t_{jl}} K_{ji} g_{ji}(t - t_{jl}) \quad (4)$$

Here, each $K_{ij} \in \mathbb{R}$, and $\mathbf{K} = \{K_{ij}\}$ where $i, j = 1 \dots M$. When $K_{ij} > 0$ we talk about excitation as above, when $K_{ij} < 0$ we call this inhibition. However, any point process requires, by design, a non-negative intensity function at every $t \in [0, T_{max}]$. We therefore now discuss two approaches to ensure this in Section 3.2.

3.2 Non-Negative Intensity

As the K_{ij} in Equation 4 can be negative it is not guaranteed that the intensity always stays above zero. There are two main approaches in the literature to tackle this issue to ensure non-negativity: restricting the parameter space or using a link function to ensure positivity.

3.2.1 Restricting the Parameter Space

We can restrict the parameter space to those parameters that lead to a positive intensity function for the observed data set. In a Bayesian frame work this can be incorporated into the prior. However, this method has three fundamental shortcomings: potential non-consistency, sampling issues, and data-dependency.

Firstly, in many applications we see an intensity function that exhibits many spikes and drops with short, rapid changes. Excluding all parameter combinations that lead to a decrease below zero *somewhere* would substantially restrict the parameter space, where many parameter combinations are prohibited. This could potentially exclude the true parameters if inhibition is truly present, which would lead to a non-consistent estimation procedure. Secondly, restricting the parameter space can cause sampling issues as MCMC samplers are prone to boundary artefacts under such conditions. Thirdly, the ‘permissibility’ of a parameter combination depends on the data. A set of parameters causing a non-negative intensity on a data set does not guarantee this property when more data is collected.

3.2.2 Link Function

Instead, a link function $\phi(\cdot)$ is commonly used to ensure a non-negative intensity, which leads to the following intensity:

$$\lambda_i(t) = \phi \left(\mu_i + \sum_{j=1}^M \sum_{l:t>t_{jl}} K_{ji} g_{ji}(t - t_{jl}) \right) \quad (5)$$

The link function $\phi(\cdot) : \mathbb{R} \rightarrow \mathbb{R}^+$ is needed to ensure a non-negative intensity at every t . For example, Mei and Eisner (2017) use the *softplus* function $\phi(x) = s \log(1 + \exp(x/s))$ with parameter s . One straightforward choice of ϕ is the *ReLU* function where $\phi(x) = \max(a, x)$ for a small, non-negative a . A popular approach in the literature is to set $a = 0$ (Lemonnier and Vayatis, 2014; Lu and Abergel, 2018; Costa et al., 2020). Crucially, this choice of a link function preserves the interpretation of K_{ij} as the average number of direct offsprings (as described in Section 2.3). Moreover, we also shown in Appendix C that it retains the branching structure, even under inhibition, which is a novel contribution to the field. Hence, for the remainder of this paper we use the *ReLU* function with $\phi(x) = \max(0, x)$.

4 Implementation

The model introduced in Equation 5 with $\phi(\cdot) = \max(0, x)$ is straightforward to define, but difficult to implement as two fundamental challenges need to be overcome. First, we review approaches from the literature to assess stability (as defined in Section 4.1) and subsequently introduce a new, stronger condition. Second, we discuss the challenge of integrating the intensity function under the given model.

4.1 Stability

Due to the self-exciting behaviour of the Hawkes process it is possible that an infinite number of events take place in finite time. For example, this can happen in a one-dimensional Hawkes-process if each event has more on average one or more offsprings. This behaviour is called *supercritical* (Helmstetter and Sornette, 2002) or *explosive* (Browning et al., 2021). However, for real-life applications it can be desirable to limit the parameter space to non-explosive instances (Kolev and Ross, 2019). This is referred to as *stability* (Brenaud and Massoulié, 1996; Bacry et al., 2020), i.e. there exists a unique stationary distribution with finite average intensity (Sulem et al., 2021).

Two conditions (**C1**, **C2** defined below) have been used in the literature to determine stability, as outlines in Section 4.1.1. In Section 4.1.2 we introduce a new condition that is stronger than both of the previously used ones. We prove that when at least one of

(**C1**, **C2**) hold, so does our condition. Moreover, there exist parameters \mathbf{K} for which our condition holds when neither of (**C1**, **C2**) do. This permits us to have a unified approach for checking stability and to classify a larger set of parameters as stable. We also provide a toy-example to illustrate this usefulness of our suggested condition.

We introduce the following notations: $\text{abs}(\mathbf{A})$ is an $M \times M$ matrix where each entry is $|A_{ij}|$, the absolute value of A_{ij} . Moreover, \mathbf{A}^+ is the matrix with entries $\max(A_{ij}, 0)$. We write $\rho(\mathbf{A})$ for the spectral radius of matrix \mathbf{A} , i.e. the largest absolute eigenvalue of matrix \mathbf{A} .

4.1.1 Stability Conditions in the Literature

To start, we state two condition to assess stability that have been introduced in the literature:

C1 A Hawkes process is stable if $\rho(\text{abs}(\mathbf{K})) < 1$ (Bremaud and Massoulié, 1996).

C2 A Hawkes process is stable if $\max_j \sum_{i=1}^M K_{ij}^+ < 1$ (Sulem et al., 2021).

Note that **C1** uses the spectral radius of the absolute value matrix, whereas **C2** utilises only the positive part of the matrix \mathbf{K} . Both conditions are sufficient, but not necessary. Sulem et al. (2021) discuss both **C1** and **C2**, but do not compare them as neither is stronger than the other. As **C1** uses the absolute value matrix, negative entries (inhibition) are converted into excitation. Hence, while the intensity is decreased by certain events, stability is check as if those events increased the intensity. Of course, this procedure is sufficient, but the intensity $\lambda_m(\cdot | \text{abs}(\mathbf{K}))$ may be rather different than the original $\lambda_m(\cdot | \mathbf{K})$, in particular when strong inhibition is present. Hence, we found there to be scope to develop a new criterion that is more closely tailored to processes that contain inhibition.

4.1.2 Introducing a New Condition

We propose a new condition to assess stability for a given parameter \mathbf{K} :

Theorem 1 (C3). *If $\rho(\mathbf{K}^+) < 1$, then the process with intensities $\lambda_m(\cdot | \mathbf{K})$, $m = 1 \dots M$, is stable.*

To prove it, we state an auxiliary lemma.

Lemma 2. *Suppose a process with intensity $\bar{\lambda}(\cdot)$ is stable. Then a process with intensity $\lambda(\cdot)$ such that $\bar{\lambda}(x) \geq \lambda(x)$ for all $x \geq 0$ is also stable.*

Proof. The stable process with intensity $\bar{\lambda}(\cdot)$ has a finite average intensity and $\bar{\lambda}(x) \geq \lambda(x)$ holds for all $x \geq 0$. The average intensity of $\lambda(\cdot)$ is therefore at most as large as the average intensity of $\bar{\lambda}(\cdot)$. Hence, the average intensity of $\lambda(x)$ is also finite and the process with intensity $\lambda(x)$ is also stable. \square

Using this lemma we now prove Theorem 1.

Proof. Since $K_{ij}^+ \geq K_{ij}$ for each $i, j = 1 \dots M$, it follows that $\lambda_m(t | \mathbf{K}^+) \geq \lambda_m(t | \mathbf{K})$ for all $m = 1 \dots M$ and all $t \in [0, T_{max}]$. By Lemma 2, if a process with intensity $\lambda_m(\cdot | \mathbf{K}^+)$ is stable then a process with intensity $\lambda_m(\cdot | \mathbf{K})$ is stable as well. A multivariate process is stable if the intensity in each dimension $m = 1 \dots M$ has finite average. If $\rho(\mathbf{K}^+) < 1$ then the multivariate process with intensities $\lambda_m(\cdot | \mathbf{K}^+)$, $m = 1 \dots M$, is stable, and therefore the multivariate process with intensities $\lambda_m(\cdot | \mathbf{K})$, $m = 1 \dots M$, is stable as well. \square

4.1.3 Comparison

We now compare **C3** to either of the existing conditions (**C1**, **C2**) and show that if at least one of them holds, so does **C3**. Moreover, there are examples where only **C3** holds. This implies that **C3** can confirm stability for more parameters, which is useful when fitting a multivariate Hawkes process.

Theorem 3. *When **C1** holds, then **C3** holds as well.*

We first state the following lemma.

Lemma 4. *Let X be a $N \times N$ matrix with entry X_{ij} in row i and column j . Then $\rho(X) \leq \max_j \sum_{i=1}^N X_{ij}$.*

This is a direct consequence of the Gelfand formula (Gelfand, 1941).

With that, we can now provide the proof for the stated Theorem 3.

Proof. First we compare **C3** to **C1** when all entries K_{ij} are non-negative (i.e. excitation only). It is trivial to see that when **C1** holds, then **C3** holds as well since $\text{abs}(\mathbf{K}) = \mathbf{K} = \mathbf{K}^+$ and therefore $\rho(\mathbf{K}^+) < 1$.

When we do not restrict the entries K_{ij} to non-negative, we note that each entry of $\text{abs}(\mathbf{K})$ is at least as large as the corresponding entry in \mathbf{K}^+ . Within the entry-wise positive matrices, the spectral radius is monotonous (Lemma 12, p. 153 Serre, 2002). Hence, if $\rho(\text{abs}(\mathbf{K})) < 1$ then also $\rho(\mathbf{K}^+) < 1$.

Therefore, when **C1** holds, then **C3** holds as well. \square

Theorem 5. *When **C2** holds, then **C3** holds as well.*

Proof. By Lemma 4, if $\max_j \sum_{i=1}^N K_{ij} < 1$ then also $\rho(\mathbf{K}^+) < 1$ and therefore **C3** holds if **C2** holds. \square

Hence, we have shown that if at least one of (**C1**, **C2**) holds, so does **C3**. In addition, there are examples where neither of the existing conditions could confirm stability, but

by using **C3** we can verify that the process is stable. Let us examine a two-dimensional Hawkes process with

$$\mathbf{K} = \begin{pmatrix} 0.5 & 1 \\ -2 & 0.5 \end{pmatrix}$$

as an illustrative example. Note that $\rho(\text{abs}(\mathbf{K})) > 1$ and the maximum column sum of \mathbf{K}^+ is also larger than 1, hence neither **C1** nor **C2** hold. Hence, by just using the two existing conditions it is not possible to assess whether a process using \mathbf{K} would be stable. However we can make use of **C3**, as $\rho(\mathbf{K}^+) < 1$ and confirm that a process using \mathbf{K} is stable.

In summary, **C3** not only provides a unified approach to assess stability, it also permits us to determine stability for more parameters than by just using (**C1**, **C2**).

4.2 Integrating the Intensity

Many parameter estimation methods, such as our subsequent Bayesian procedures, need to evaluate the likelihood (Equation 3). However, this requires Λ , the integral of the intensity function. While this is straightforward task in an excitation-only Hawkes process, more deliberation is required for the more general model introduced in Section 3.1. We discuss different approaches from the literature, present exact solutions for particular choices of the influence kernel, and suggest an approximate solution that will be subsequently utilised.

When all K_{ij} are non-negative and $\phi(x) = x$, the integral of the intensity can be computed by integrating each segment between events (as well as the ones between 0 and the first event and between the last event and T_{max}). This reduces to an easy computation of the integral that sums over the background rate and the contributions of each event (Ogata, 1981). However, it becomes difficult to integrate the intensity function under inhibition in this scenario as the intensity might drop below zero. Lu and Abergel (2018) choose to calculate the integral as in the excitation-only case, even though the parts of the integral below zero contributing negatively to the integral.

The use of a link function $\phi(\cdot)$ guarantees a non-negative intensity function (see Section 3.2.2). However, any choice of link that is not the identity prohibits a straightforward calculation of the integral as the approach by Ogata (1981) cannot be employed anymore. Mei and Eisner (2017) explain in their supplementary materials that they approximate Λ for a one-dimensional Hawkes process by sampling one t^* uniformly from $[0, T_{max}]$ and then use $\hat{\Lambda} = T_{max}\lambda(t^*)$. While $\hat{\Lambda}$ is indeed an unbiased estimator for Λ it has a large variance. The intensity functions often exhibit rapid ups and downs, such that just evaluating it once cannot capture all aspects of the function. Ertekin et al. (2015) use Approximate Bayesian Computation to circumvent the problem as this method does not require an evaluation of the likelihood and therefore the integral is not required.

Another possibility is to identify the intervals of the intensity function that are non-negative and integrate those only, which corresponds to setting $\phi(x) = \max(0, x)$. While this is an exact solution, this approach requires finding the roots of the intensity function, which depend on the exact specifications of the model. A popular choice for the influence kernel is the exponential kernel $g_{ij}(x) = \beta_{ij} \exp(-\beta_{ij} x)$ (e.g. Blundell et al., 2012; Shelton et al., 2018). In Appendix A.2 we show that the roots of the intensity function with this kernel are the solutions to a high-order polynomial. The computational complexity of this root finding approach is high since the root-finding needs to be employed between each event time in every dimension. When setting all β_{ij} to be equal, we find a simple expression for the roots when using the exponential kernel, as shown in Appendix A.1. However, this assumption may be too restrictive in application.

For our example we resort to a numerical approximation of Λ without placing any restrictions on β_{ij} . In each segment between events in every dimension we use a Simpson’s rule approximation, for details see Appendix B. In trial runs on simulated data we found this cubic approximation (‘3/8 Simpson’s rule’) to provide a good approximation, albeit with four intensity evaluations per segment. While this is a costly approximation in terms of computational complexity, any lower level approximation introduced too much bias, and yet the cubic approximation is faster than solving a polynomial in each interval.

5 Prior Choice

To implement the proposed model in a Bayesian framework we investigate prior choices. Throughout the literature Hawkes processes are parameterised in terms of \mathbf{K} . For example, Browning et al. (2021) choose a uniform prior for each of its entries. However, when the dimension M is large the non-negative entries of \mathbf{K} have to be smaller in order to retain stability in accordance the criteria outlined in Section 4.1. For example, when all entries of \mathbf{K} are 0.4, a two-dimensional process is stable, whereas a three-dimensional \mathbf{K} has an eigenvalue larger than one. Hence, in a Bayesian framework priors on \mathbf{K} would have to be adapted according to the dimension M .

Instead, we suggest to reparametrise the model to circumvent this problem using the total number of offsprings, which does not suffer from this dimension-dependency. In the following sections we define this quantity and subsequently use it to parametrise the problem, such that normal priors and sparsity-inducing horseshoe priors can be employed.

5.1 Reparametrise the Model Using the Total Number of Offsprings

We now formally define the total number of offsprings. First, we assume that all entries of \mathbf{K} are non-negative. Section 2.3 introduces the notion of direct offspring, i.e. an event

in dimension j from the immigrant process of an event in dimension i . However, when estimating the parameters it can become difficult to distinguish between an event in i triggering an immigrant process in dimension j ($i \rightarrow j$) and an event in i triggering an immigrant process in dimension k , which produces an event that, in turn, triggers an immigrant process in j ($i \rightarrow k \rightarrow j$). This problem is perpetuated further in higher dimensions (Eichler, 2013). We therefore propose to investigate the total number of offsprings that circumvents this issue. For this, two kinds of events are defined as an indirect offspring of event t_i :

1. an event from an immigrant process that was triggered by a direct offspring of t_i
2. an event from an immigrant process that was triggered by an indirect offspring of t_i

We define K_{ij}^* as the total number of offsprings an event in dimension i has in dimension j , which is calculated as the sum of direct and indirect offsprings. We write $\mathbf{K}^* = \{K_{ij}^*\}$ where $i, j = 1 \dots M$.

Theorem 6. *The total number of offsprings is*

$$\mathbf{K}^* = (I - \mathbf{K})^{-1} - I$$

The proof is available in Appendix D. It is important to note that the idea and definition of \mathbf{K}^* have already been presented in the literature, but not in a unified concept towards use in application. On one hand, Bacry and Muzy (2016) introduce this formula without its interpretation in the context of a matrix convolution. On the other hand, Bacry et al. (2016) define the concept of total offsprings but do not provide a closed form expression. Crucially, neither of them make extensive use of the concept.

If a process is stable (see Section 4.1), the calculation remains the same when entries of \mathbf{K} are negative and \mathbf{K}^* still provides meaningful interpretation. While positive entries of \mathbf{K}^* describe the average number of total offsprings, a negative entry summarises the *negative contributions* to the intensity function across dimensions. The number of actually inhibited events depends on the number of events in the process. Nevertheless, \mathbf{K}^* retains its attractive interpretation and can be used to place priors without having to consider the dimensions M .

Crucially, the entries of \mathbf{K}^* for a stable process are not dependent on the dimension M . For the example in Section 7 we therefore reparameterise the multivariate Hawkes process in terms of \mathbf{K}^* such that the intensity for dimension i is written as:

$$\lambda_i(t) = \phi \left(\mu_i + \sum_{j=1}^M \sum_{l:t>t_{jl}} \{f(\mathbf{K}^*)\}_{ji} g_{ji}(t - t_{jl}) \right) \quad (6)$$

where $f(\mathbf{X}) = I - (\mathbf{X} - I)^{-1}$.

5.2 Normal Priors

This reparametresation in Equation 6 permits us to use priors directly for \mathbf{K}^* and write the model already in the quantity of interest. We restrict the parameter space of \mathbf{K}^* such that only stable parameters (according to **C3**) are allowed. One option is to place independent normal priors on each entry of \mathbf{K}^* :

$$K_{ij}^* \sim \mathcal{N}(0, 1) \quad \text{for } i, j = 1 \dots M \text{ (stable only)} \quad (7)$$

5.3 Sparsity Priors

Many real life problems of multivariate Hawkes processes contain sparsity (see Section 2.2, which we wish to reflect in our model. As mentioned in Section 5, when M is large, the positive entries of \mathbf{K} have to be small in order to retain stability (according to **C3** in Section 4.1). When employing shrinkage strategies in larger dimensions it can therefore be difficult to distinguish between small non-zero entries of \mathbf{K} and truly zero ones.

For our example we therefore choose to place horseshoe priors independently on each K_{ij}^* , which shrink small values towards zero but leave larger values untouched (Carvalho et al., 2009):

$$\begin{aligned} \xi_{ij} &\sim \text{Cauchy}(0, 1) & (8) \\ K_{ij}^* &\sim \mathcal{N}(0, \xi_{ij}) & \text{for } i, j = 1 \dots M \text{ (stable only)} & (9) \end{aligned}$$

6 Posterior Inference

To summarise the above, we fit the following multivariate Hawkes process in a Bayesian manner. The intensity in dimension i is

$$\lambda_i(t) = \phi \left(\mu_i + \sum_{j=1}^M \sum_{l:t>t_{jl}} \{g(\mathbf{K}^*)\}_{ji} g_{ji}(t - t_{jl}) \right) \quad (10)$$

with link function

$$\phi(x) = \max(0, x) \quad (11)$$

The likelihood is

$$p(Y) = \prod_{m=1}^M \prod_{i=1}^{N_m} \lambda_m(t_i | \theta) \exp(-\Lambda) \quad (12)$$

where $\Lambda = \sum_{m=1}^M \int_0^{T_{max}} \lambda_m(x) dx$. The following priors are chosen for the background rate:

$$\mu_i \sim \mathcal{U}(0, 10) \quad \text{for } i = 1 \dots M \quad (13)$$

We found that in practice prior knowledge is often available to find sensible upper bounds for these uniform priors. For example the magnitude of number of events can help guide the priors for μ_i .

For the influence kernels we utilise the popular exponential kernel $g_{ij}(x) = \beta_{ij} \exp(-\beta_{ij} x)$ (e.g. Blundell et al., 2012; Shelton et al., 2018). Here, we assume that all $\beta_{ii} = \beta_{diag}$ and $\beta_{ij} = \beta_{off}$ when $i \neq j$. Hence, the values for are the same for all self-influences, as well as cross-influences, respectively. For β_{diag} and β_{off} we choose the following priors.

$$\beta_{diag} \sim \mathcal{U}(0, 3) \tag{14}$$

$$\beta_{off} \sim \mathcal{U}(0, 3) \tag{15}$$

In line with the arguments from Section 5.1 we place priors on the entries of \mathbf{K}^* . The estimation is carried out both using Normal and sparsity inducing priors (using the horseshoe prior from Section 5.3). First, we use Normal priors:

$$K_{ij}^* \sim \mathcal{N}(0, 1) \quad \text{for } i, j = 1 \dots M \text{ (stable only)} \tag{16}$$

In addition, we also fit the model with the horseshoe prior (Carvalho et al., 2009):

$$\xi_{ij} \sim \text{Cauchy}(0, 1) \tag{17}$$

$$K_{ij}^* \sim \mathcal{N}(0, \xi_{ij}) \quad \text{for } i, j = 1 \dots M \text{ (stable only)} \tag{18}$$

We use Stan (Stan Development Team, 2019) to obtain posterior samples from this probabilistic model. As each evaluation of the likelihood requires Λ , the integration of the likelihood, we implement a cubic Simpson’s rule to approximate the integral of the intensity function between each event (see Section 4.2 and Appendix B). To analyse the posterior we generate density plots and summary statistics.

7 Example

This section showcases one example of a multivariate Hawkes process with excitation and inhibition using the set up from Section 6. We simulate a data set for $M = 3$ dimensions using the following parameter values for $\Theta = (\mu, \mathbf{K}^*, \beta_{diag}, \beta_{off})$.

$$\begin{aligned} \mu &= (0.15, 0.15, 0.15) \\ \mathbf{K}^* &= \begin{pmatrix} 0.3 & -0.3 & 0 \\ 0 & 0.3 & 0.3 \\ 0 & -0.3 & 0 \end{pmatrix} \\ \beta_{diag} &= \beta_{off} = 0.5 \end{aligned}$$

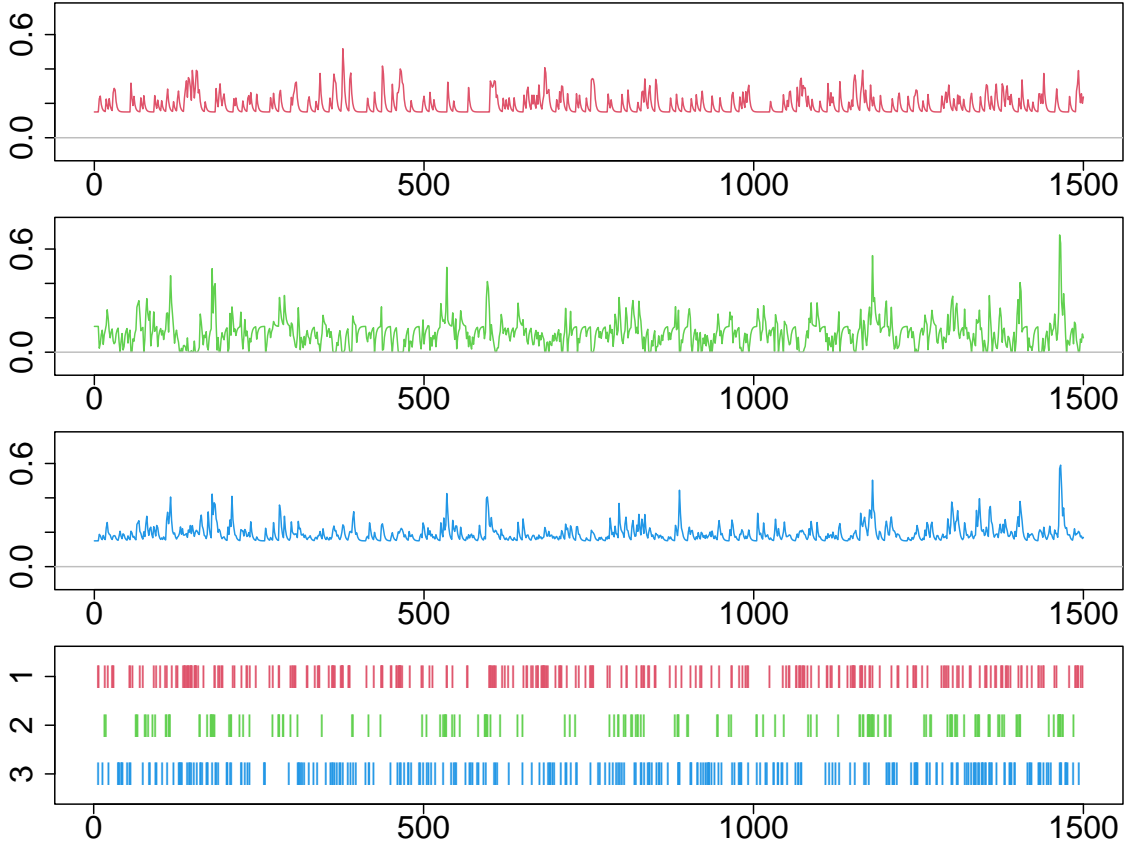


Figure 2: Intensity functions for each dimension under the true parameters in the first three panels and observations on the bottom panel.

Data is generated for the interval $[0, T_{max} = 1, 500]$, resulting in 714 observations, (275, 162, and 277 for each dimension). Figure 2 displays the intensity functions for each dimension under the generating parameters alongside the events themselves.

The estimation is carried out both using normal priors and sparsity-inducing horseshoe prior from Section 5.3. Figure 3 displays the posterior estimates based on 750 samples obtained by Stan (Stan Development Team, 2019). Table 1 summarises the posterior means (and standard deviations) for both models. Most posterior distributions are centred around the parameter used for sampling, only \mathbf{K}_{22}^* is not covered well. Generally, both models are successful in recovering the parameters, given that it is a rather challenging task to estimate 14 heavily intertwined parameters with just 714 observations.

The horseshoe prior gives similar results as the Normal priors. As expected, the horseshoe posteriors have less variance when the true value is actually zero. For example the posterior mean in the Normal case for $K_{31}^* = 0$ is -0.03 (0.07), whereas the horseshoe posterior mean is -0.01 (0.06). This can help to identify truly zero entries in the \mathbf{K}^* matrix.

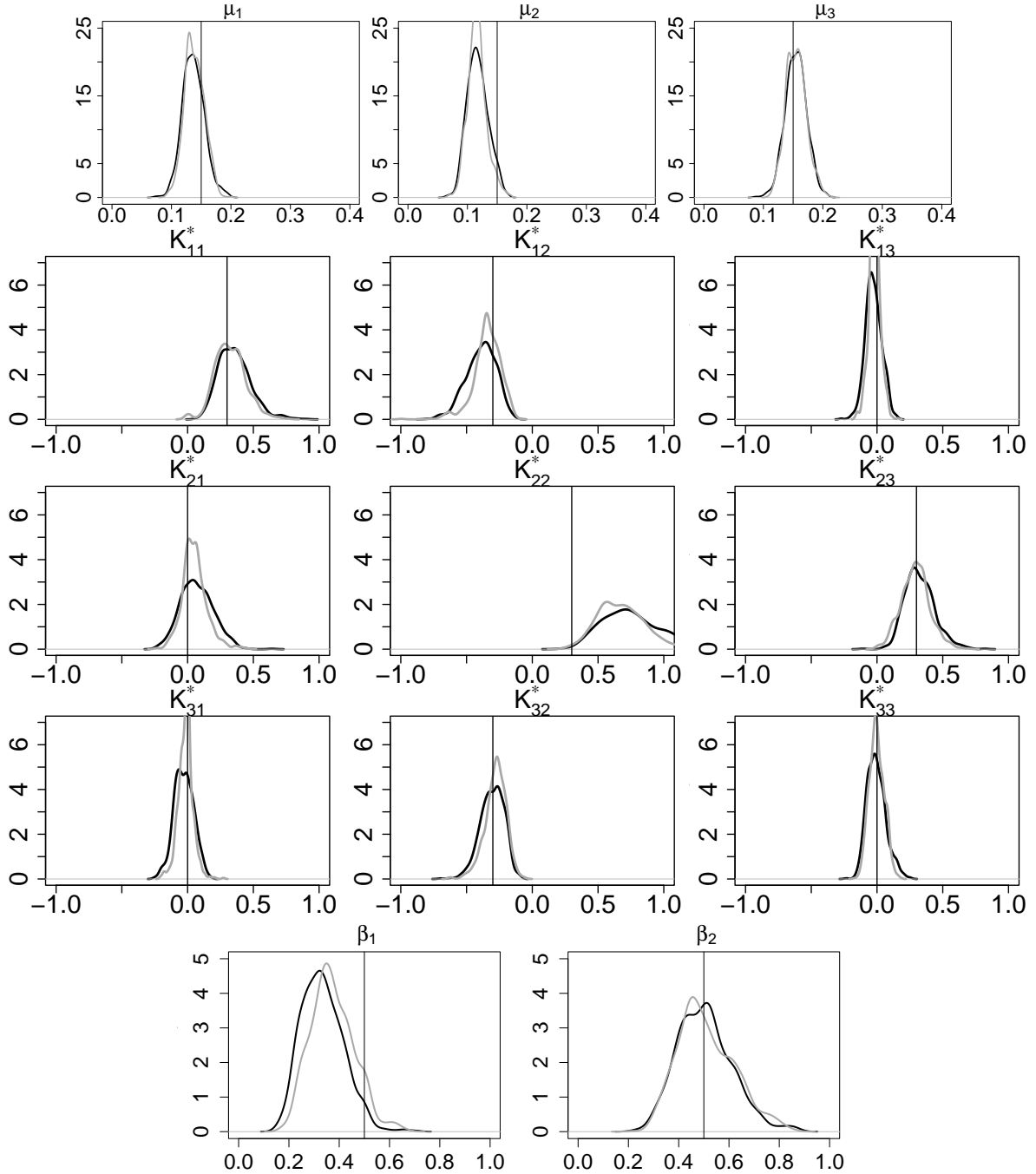


Figure 3: Posterior estimates for all parameters. Black lines are for Normal priors, grey for horseshoe priors. Vertical line indicates the true value.

8 Discussion

In this paper we focused on the multivariate Hawkes process under both excitation and inhibition. We discussed methodological aspects of the model and introduced a new, stronger stability criterion. We also showed that the branching structure can be retained even under inhibition. We examined prior selection in a Bayesian framework using a reparametrisation based on the total number of events. The resulting Normal and sparsity

Table 1: Posterior mean (and standard deviation) rounded to two decimal places for each parameter for two models: using Normal priors and a shrinkage approach (using the horseshoe prior).

	true	Normal	horseshoe
μ_1	0.15	0.14 (0.02)	0.14 (0.02)
μ_2	0.15	0.12 (0.02)	0.12 (0.02)
μ_2	0.15	0.15 (0.02)	0.16 (0.02)
K_{11}^*	0.30	0.36 (0.12)	0.33 (0.12)
K_{21}^*	0.00	0.07 (0.12)	0.05 (0.09)
K_{31}^*	0.00	-0.03 (0.07)	-0.01 (0.06)
K_{12}^*	-0.30	-0.39 (0.11)	-0.34 (0.10)
K_{22}^*	0.30	0.77 (0.24)	0.70 (0.22)
K_{32}^*	-0.30	-0.31 (0.09)	-0.28 (0.08)
K_{13}^*	0.00	-0.03 (0.06)	-0.02 (0.05)
K_{23}^*	0.30	0.33 (0.11)	0.29 (0.11)
K_{33}^*	0.00	0.00 (0.07)	0.00 (0.06)
β_{diag}	0.50	0.33 (0.08)	0.37 (0.09)
β_{off}	0.50	0.50 (0.11)	0.51 (0.11)

priors where then showcased on an example on simulated data.

Our work can be extended by considering different link functions and a variety of influence kernels, or differently structured inhibition altogether (for example along the lines of Apostolopoulou et al., 2019). Moreover, all stability conditions, including our newly proposed **C3**, are only sufficient to check stability. It would be of great interest to develop a criterion that was both necessary and sufficient.

Future work will be carried out on real-world data for one of the many attractive applications of Hawkes processes with inhibition. Moreover, we would like to extend the applications to higher dimensions and to incorporate additional covariate information.

References

- Apostolopoulou, I., Linderman, S., Miller, K., and Dubrawski, A. (2019). Mutually regressive point processes. In *Advances in Neural Information Processing Systems*, volume 32. Curran Associates, Inc.
- Bacry, E., Bompain, M., Gaïffas, S., and Muzy, J.-F. (2020). Sparse and low-rank multivariate Hawkes processes. *Journal of Machine Learning Research*, 21(50):1–32.
- Bacry, E., Jaisson, T., and Muzy, J. (2016). Estimation of slowly decreasing Hawkes

- kernels: application to high-frequency order book dynamics. *Quantitative Finance*, 16(8):1179–1201.
- Bacry, E. and Muzy, J.-F. (2016). First-and second-order statistics characterization of Hawkes processes and non-parametric estimation. *IEEE Transactions on Information Theory*, 62(4):2184–2202.
- Blundell, C., Beck, J., and Heller, K. A. (2012). Modelling reciprocating relationships with Hawkes processes. *Advances in Neural Information Processing Systems*, 25:2600–2608.
- Bremaud, P. and Massoulié, L. (1996). Stability of nonlinear Hawkes processes. *The Annals of Probability*, 24(3):1563–1588.
- Browning, R., Sulem, D., Mengersen, K., Rivoirard, V., and Rousseau, J. (2021). Simple discrete-time self-exciting models can describe complex dynamic processes: A case study of COVID-19. *PLOS ONE*, 16(4):e0250015.
- Carvalho, C. M., Polson, N. G., and Scott, J. G. (2009). Handling sparsity via the horseshoe. In *Artificial Intelligence and Statistics*, pages 73–80. PMLR.
- Chen, F. and Stindl, T. (2018). Direct likelihood evaluation for the renewal Hawkes process. *Journal of Computational and Graphical Statistics*, 27(1):119–131.
- Costa, M., Graham, C., Marsalle, L., and Tran, V.-C. (2020). Renewal in Hawkes processes with self-excitation and inhibition. *Advances in Applied Probability*, 52(3):879–915.
- Daley, D. J. and Vere-Jones, D. (2003). *An Introduction to the Theory of Point Processes: Volume I: Elementary Theory and Methods*. Probability and Its Applications, An Introduction to the Theory of Point Processes. Springer-Verlag, New York, NY, 2 edition.
- Eichler, M. (2013). Causal inference with multiple time series: principles and problems. *Philosophical Transactions of the Royal Society A: Mathematical, Physical and Engineering Sciences*, 371(1997):20110613.
- Eichler, M., Dahlhaus, R., and Dueck, J. (2017). Graphical modeling for multivariate Hawkes processes with nonparametric link functions. *Journal of Time Series Analysis*, 38(2):225–242.
- Ertekin, Ş., Rudin, C., and McCormick, T. H. (2015). Reactive point processes: A new approach to predicting power failures in underground electrical systems. *The Annals of Applied Statistics*, 9(1):122–144.

- Gelfand, I. (1941). Normierte ringe. *Rech. Math. [Mat. Sbornik]*, 9(1):3–24.
- Guo, X., Hu, A., Xu, R., and Zhang, J. (2018). Consistency and computation of regularized MLEs for multivariate Hawkes processes. *arXiv:1810.02955 [math, stat]*.
- Hawkes, A. G. (1971). Spectra of some self-exciting and mutually exciting point processes. *Biometrika*, 58(1):83–90.
- Hawkes, A. G. and Oakes, D. (1974). A cluster process representation of a self-exciting process. *Journal of Applied Probability*, 11(3):493–503.
- Helmstetter, A. and Sornette, D. (2002). Subcritical and supercritical regimes in epidemic models of earthquake aftershocks. *Journal of Geophysical Research: Solid Earth*, 107(B10):ESE 10–1–ESE 10–21.
- Jovanović, S., Hertz, J., and Rotter, S. (2015). Cumulants of Hawkes point processes. *Physical Review E*, 91(4):042802.
- Kalair, K., Connaughton, C., and Alaimo Di Loro, P. (2021). A non-parametric Hawkes process model of primary and secondary accidents on a UK smart motorway. *Journal of the Royal Statistical Society: Series C (Applied Statistics)*, 70(1):80–97.
- Kolev, A. A. and Ross, G. J. (2019). Inference for etas models with non-poissonian mainshock arrival times. *Statistics and Computing*, 29(5):915–931.
- Lai, E. L., Moyer, D., Yuan, B., Fox, E., Hunter, B., Bertozzi, A. L., and Brantingham, P. J. (2016). Topic time series analysis of microblogs. *IMA Journal of Applied Mathematics*, 81(3):409–431.
- Lemonnier, R. and Vayatis, N. (2014). Nonparametric markovian learning of triggering kernels for mutually exciting and mutually inhibiting multivariate hawkes processes. In *Proceedings of the 2014th European Conference on Machine Learning and Knowledge Discovery in Databases - Volume Part II*, page 161–176, Berlin, Heidelberg. Springer-Verlag.
- Lu, X. and Abergel, F. (2018). High-dimensional hawkes processes for limit order books: modelling, empirical analysis and numerical calibration. *Quantitative Finance*, 18(2):249–264.
- Mei, H. and Eisner, J. (2017). The neural Hawkes process: A neurally self-modulating multivariate point process. In *Advances in Neural Information Processing Systems*, volume 30, page 6757–6767. Curran Associates Inc.

- Miscouridou, X., Caron, F., and Teh, Y. W. (2018). Modelling sparsity, heterogeneity, reciprocity and community structure in temporal interaction data. In *Advances in Neural Information Processing Systems*, volume 31. Curran Associates, Inc.
- Mohler, G. (2013). Modeling and estimation of multi-source clustering in crime and security data. *The Annals of Applied Statistics*, 7(3):1525–1539.
- Ogata, Y. (1981). On Lewis’ simulation method for point processes. *IEEE Transactions on Information Theory*, 27(1):23–31.
- Ogata, Y. (1988). Statistical models for earthquake occurrences and residual analysis for point processes. *Journal of the American Statistical Association*, 83(401):9–27.
- Rambaldi, M., Bacry, E., and Lillo, F. (2017). The role of volume in order book dynamics: a multivariate Hawkes process analysis. *Quantitative Finance*, 17(7):999–1020.
- Rasmussen, J. G. (2013). Bayesian inference for Hawkes processes. *Methodology and Computing in Applied Probability*, 15(3):623–642.
- Serre, D. (2002). *Matrices: Theory and Applications*. Springer Science & Business Media, New York, NY, 2 edition.
- Shelton, C., Qin, Z., and Shetty, C. (2018). Hawkes process inference with missing data. *Proceedings of the Thirty-Second AAAI Conference on Artificial Intelligence*.
- Stan Development Team (2019). RStan: the R interface to Stan. R package version 2.19.2.
- Sulem, D., Rivoirard, V., and Rousseau, J. (2021). Bayesian estimation of nonlinear Hawkes process. *arXiv:2103.17164 [math, stat]*.
- Tetereva, A. (2018). Do financial companies communicate to one another in the news? (application of multivariate hawkes graphs to uncover granger causality of financial news). *Econometric Modeling: Capital Markets - Asset Pricing eJournal*.
- Tucker, D. J., Shand, L., and Lewis, J. R. (2019). Handling missing data in self-exciting point process models. *Spatial Statistics*, 29:160–176.
- Veen, A. and Schoenberg, F. P. (2008). Estimation of space-time branching process models in seismology using an em-type algorithm. *Journal of the American Statistical Association*, 103(482):614–624.
- Xu, H., Farajtabar, M., and Zha, H. (2016). Learning Granger causality for Hawkes processes. In *International Conference on Machine Learning*, pages 1717–1726. PMLR.

Yu, X., Shanmugam, K., Bhattacharjya, D., Gao, T., Subramanian, D., and Xue, L. (2020). Hawkesian Graphical Event Models. In *International Conference on Probabilistic Graphical Models*, pages 569–580. PMLR.

Appendices

A Roots of the Intensity Function

This section shows how the roots of the intensity function can be found when using the exponential kernel. As described in Section 4.2, these can be used to calculate the integral of the intensity exactly.

A.1 Exponential Kernel with All β_{ij} Equal

We start with a special case where all β_{ij} are equal and examine the roots both in one dimension and M dimensions.

A.1.1 One Dimension

Assume that we have data $Y = (t_1 \dots t_N)$ from one dimension and the intensity function is defined with the exponential kernel:

$$\lambda(t) = \mu + \sum_{i:t>t_i} K \beta \exp(-\beta(t - t_i)) \quad (19)$$

The intensity can only drop below zero when an event happens. Therefore it is sufficient to check only intervals after an event at which the intensity is negative to see if the intensity becomes positive again before the next event happens.

Then we can find the root t between observation t_n and t_{n+1} in the following way:

$$\begin{aligned} \mu + \sum_{i=1}^n K \beta \exp(-\beta(t - t_i)) &= 0 \\ \mu + \sum_{i=1}^n K \beta \exp(-\beta t) \exp(\beta t_i) &= 0 \\ \exp(-\beta t) \left[\sum_{i=1}^n K \beta \exp(\beta t_i) \right] &= -\mu \\ t &= \frac{\log\left(\frac{-\mu}{\sum_{i=1}^n K \beta \exp(\beta t_i)}\right)}{-\beta} \end{aligned}$$

if $t_n < t < t_{n+1}$.

A.1.2 M Dimensions

Now assume we have M dimensional data $Y_1 = (t_{11} \dots t_{1N_1}) \dots Y_M = (t_{M1} \dots t_{MN_M})$ with intensity function

$$\lambda_i(t) = \mu_i + \sum_{j=1}^M \sum_{q:t>t_{qi}} K_{ji} g_{ji}(t - t_{jl}) \quad (20)$$

Again, we only intervals after an event at which the intensity would be negative to see if the intensity becomes positive again before the next event happens. However, we need to check in each interval in each dimension.

To check in dimension m after an observation t_n from arbitrary dimension we can start with

$$\mu_m + \sum_{q=1}^M \sum_{i:t_{qi}<t_n} K_q \beta \exp(-\beta(t - t_{qi})) = 0$$

which leads to the following expression for the root

$$t = \frac{\log \left(\frac{-\mu_m}{\sum_{q=1}^M \sum_{i:t_{qi}<t_n} K_q \beta \exp(\beta t_{qi})} \right)}{-\beta}$$

if $t_n < t < t_{n+1}$.

A.2 General Exponential Kernel

Now we examine the general case when all betas are different. Here, finding the roots is a polynomial problem:

$$\begin{aligned} \mu_m + \sum_{q=1}^M \sum_{i:t_{qi}<t_n} K_q \beta_q \exp(-\beta_q(t - t_{qi})) &= 0 \\ \mu_m + \sum_{q=1}^M \sum_{i:t_{qi}<t_n} K_q \beta_q u^{-\beta_q} \exp(\beta_q t_{qi}) &= 0 \text{ where } x = \exp(t) \\ \mu_m + \sum_{q=1}^M x^{-\beta_q} \underbrace{\sum_{i:t_{qi}<t_n} K_q \beta_q \exp(\beta_q t_{qi})}_{v_q} &= 0 \\ \mu_m + \sum_{q=1}^M x^{-\beta_q} v_q &= 0 \end{aligned}$$

This is now a polynomial in x that needs to be solved.

B Approximating Λ using the Simpson's Rule

This section describes the approximation procedure for $\Lambda = \sum_{m=1}^M \int_0^{T_{max}} \lambda_m(x) dx$ as mentioned in Section 4.2. We use the Cubic Simpson's Rule where

$$\int_a^b f(x) dx \approx \frac{(b-a)}{8} \left[f(a) + 3f\left(\frac{2a+b}{3}\right) + 3f\left(\frac{a+2b}{3}\right) + f(b) \right] \quad (21)$$

Assume we have M dimensional data $Y_1 = (t_{11} \dots t_{1N_1}) \dots Y_M = (t_{M1} \dots t_{MN_M})$ and intensity function $\lambda_m(\cdot)$ for each dimension $m = 1 \dots M$. Algorithm 1 outlines the approximation procedure used.

Algorithm 1 Approximating Λ using the Simpson's Rule

- 1: Set $Y_{total} = (0, t_{11} \dots t_{1N_1} \dots t_{M1} \dots t_{MN_M}, T_{max})$
 - 2: Order all entries of Y_{total} and call the result $X = (x_1 < \dots < x_P)$ where $P = 2 + \sum_m N_m$
 - 3: Define $X^t = \{x_i : x_i \leq t\}$
 - 4: Set $res = 0$
 - 5: **for** i in $1 : (P - 1)$ **do**
 - 6: Set $a = x_i$
 - 7: Set $b = x_{i+1}$
 - 8: **for** m in $1 : M$ **do**
 - 9: Set $res = res + \frac{(b-a)}{8} [\lambda_m(a|X^a) + 3\lambda_m(\frac{2a+b}{3}|X^a) + 3\lambda_m(\frac{a+2b}{3}|X^a) + \lambda_m(b|X^a)]$
 - 10: **end for**
 - 11: **end for**
 - 12: Return res as the approximation of Λ
-

C Branching Structure with Inhibition

This section outlines a sampling procedure that preserves the branching structure (see Section 2.3) of a Hawkes process, even if inhibition is present.

We define the direct parent of an event as follows. If t_j is a direct offspring of t_i , then t_i is the parents of t_j . For each event t_i we define $B(t_i) = 0$ if t_i was an immigrant event. Otherwise $B(t_i)$ takes the index the direct parent of t_i . For example if t_i has one offspring t_j then $B(t_j) = i$. Moreover, let $C(t_i)$ contain all direct and indirect ('total') offsprings of t_i .

We assume that $\phi(x) = \max(0, x)$, as it ensures that $\lambda(t | \mathbf{K}^+) > \lambda(t | \mathbf{K})$ for all t .

First, we review the classic thinning approach.

Lemma 7. *Let $X = (x_1 \dots x_P)$ be event times from a point process with intensity $\bar{\lambda}(\cdot)$. Suppose there is another point process with intensity function $\lambda(\cdot)$ such that $\bar{\lambda}(x) \geq \lambda(x)$*

for all $x \geq 0$. To obtain samples from $\lambda(\cdot)$, take $X = (x_1 \dots x_P)$ as candidates. Let Y be the empty set. Each x_i , $i = 1 \dots P$, is added to Y with probability $\lambda(x_i)/\bar{\lambda}(x_i)$. The event times in Y are samples from the process with intensity $\lambda(\cdot)$.

This is the popular ‘thinning’ sampler for point processes, as introduced by Ogata (1981). Algorithm 2 outlines this approach, where each event is thinned independently, regardless of the branching structure. In particular, in Line 6 we calculate $b_{original}$ using all generated events in $Y_{original}$, regardless how many of those are still in Y .

Now we look at a different sampling procedure as outlines in Algorithm 3. It differs from the algorithm above in two aspects. Here, b is calculated with only the retained events (Line 8), and offsprings are removed with its parents (Line 10). Note that our sampling approach under inhibition is inherently different to the one introduced by Apostolopoulou et al. (2019) as they work with a different model set up that specifies inhibition through a multiplicative factor.

Theorem 8. *Algorithm 3 generates samples from the correct target intensity $\lambda(\cdot | \mathbf{K})$.*

Proof. Before any event is removed, the algorithm mirrors the classic thinning approach.

Let us now assume that event t_i is removed (Line 10), along with all of its offsprings, of which k lie before event t_j , which remains.

$$\begin{aligned} Y_{original} &= (t_1 \dots t_{i-1}, t_i, t_{i+1} \dots t_{i+k}, t_j, \dots) \\ Y &= (t_1 \dots t_{i-1}, t_j, \dots) \end{aligned}$$

Hence, at this point we could discard all events after t_{i-1} and instead sample from any proposal (that is larger than the target) and thin again according to the classic thinning approach. We choose to sample this new proposal event from $\lambda(\cdot | \mathbf{K}^+, \mathcal{H} = Y)$ using the branching structure. However, we have already generated such an event, namely t_j . Since t_j has not been removed, it was either an immigrant event or an offspring of an event in Y , therefore it can be viewed as sampled from the desired $\lambda(\cdot | \mathbf{K}^+, \mathcal{H} = Y)$. Hence, the ration in Line 9 follows the usual thinning procedure and Algorithm 3 describes a sampling procedure that samples from the target intensity function $\lambda(\cdot | \mathbf{K})$. \square

Crucially, all parents of events in Y are also in Y by construction. Hence the branching structure is retained, even under inhibition.

Algorithm 2 Classic Thinning Sampling without branching structure

- 1: Sample $Y_{original} = (t_1 < \dots < t_N)$ from $\lambda(\cdot | \mathbf{K}^+)$
 - 2: Set $Y = Y_{original}$
 - 3: **for** i in $1 : N$ **do**
 - 4: sample $u \sim \mathcal{U}[0, 1]$
 - 5: set $a = \lambda(t_i | \mathbf{K}, \mathcal{H} = Y)$
 - 6: set $b_{original} = \lambda(t_i | \mathbf{K}^+, \mathcal{H} = Y_{original})$
 - 7: **if** $u > a/b_{original}$ **then**
 - 8: remove t_i from Y
 - 9: **end if**
 - 10: **end for**
 - 11: Return Y as a sample from the multivariate Hawkes Process
-

Algorithm 3 Sampling with inhibition while retaining the branching structure

- 1: Sample $Y_{original} = (t_1 < \dots < t_N)$ from $\lambda(\cdot | \mathbf{K}^+)$ using branching
 - 2: Keep the $B(t_i)$ for all $i = 1 \dots N$
 - 3: Set $Y = Y_{original}$
 - 4: **for** i in $1 : N$ **do**
 - 5: **if** $t_i \notin Y$ **then** next
 - 6: **else** sample $u \sim \mathcal{U}[0, 1]$
 - 7: set $a = \lambda(t_i | \mathbf{K}, \mathcal{H} = Y)$
 - 8: set $b = \lambda(t_i | \mathbf{K}^+, \mathcal{H} = Y)$
 - 9: **if** $u > a/b$ **then**
 - 10: remove t_i and $C(t_i)$ from Y
 - 11: **end if**
 - 12: **end if**
 - 13: **end for**
 - 14: Return Y as a sample from the multivariate Hawkes Process
-

D Total Number of Offsprings

This section contains the proof of the total number of offsprings from Section 5.1.

We write K_{ij}^* is the total number of offsprings in dimension j that are produced by an event cascade started by an immigrant event in i . This can be interpreted as the *marginal* influence from i onto j as both direct and indirect influences are taken into account. We write \mathbf{K}^* where K_{ij}^* is the entry in row i and column j .

Here, $N = (N_1 \dots N_M)^T$ is the total number of events in each dimension, which can be calculated by $N = (I - \mathbf{K}^T)^{-1} \mu$, as described by Hawkes (1971); Jovanović et al. (2015).

Lemma 9. *The number of events in each dimension is*

$$N = (N_1 \dots N_M)^T = (\mathbf{K}^* + I)^T \mu$$

where I is the identity matrix of appropriate dimension M .

Proof. The Hawkes process can be written as the superposition of Poisson processes as outlined by the branching structure interpretation (see Section 2.3). Hence, each N_i consist of two parts:

1. The number of immigrants events from the background process with rate μ_i
2. The number of offsprings in i from an immigrant event in each dimension j

Therefore, we can write

$$N_i = \mu_i T_{max} + \sum_{j=1}^M \mu_j T_{max} K_{ji}^* \quad (22)$$

In matrix notation this is

$$N = (N_1 \dots N_M)^T = (\mathbf{K}^* + I)^T \mu \quad (23)$$

where I is the identity matrix of appropriate dimension M . □

Theorem 10. *The total number of offsprings is*

$$\mathbf{K}^* = (I - \mathbf{K})^{-1} - I$$

Proof. We use the definition of N from the literature

$$N = (I - \mathbf{K}^T)^{-1} \mu \quad (24)$$

and relate it to Lemma 9:

$$(I - \mathbf{K}^T)^{-1} \mu = (\mathbf{K}^* + I)^T \mu \quad (25)$$

Rearranging, this allows us to write \mathbf{K}^* as

$$\mathbf{K}^* = (I - \mathbf{K})^{-1} - I \quad (26)$$

□